

# Angular correlation and deformed Hellings-Downs curve by spin-2 ultralight dark matter

Rong-Gen Cai<sup>2,3,1,\*</sup>, Jing-Rui Zhang<sup>1,†</sup> and Yun-Long Zhang<sup>4,1,5,‡</sup>

<sup>1</sup>*School of Fundamental Physics and Mathematical Sciences,*

*Hangzhou Institute for Advanced Study, UCAS, Hangzhou 310024, China.*

<sup>2</sup>*School of Physics Sciences and Technology, Ningbo University, Ningbo, 315211, China*

<sup>3</sup>*CAS Key Laboratory of Theoretical Physics, Institute of Theoretical Physics, Chinese Academy of Sciences, Beijing 100190, China.*

<sup>4</sup>*National Astronomy Observatories, Chinese Academy of Science, Beijing, 100101, China and*

<sup>5</sup>*International Center for Theoretical Physics Asia-Pacific, Beijing/Hangzhou, China*

The pulsar timings are sensitive to both the nanohertz gravitational-wave background and the oscillation of ultralight dark matter. The Hellings-Downs angular correlation curve provides a criterion to search for stochastic gravitational-wave backgrounds at nanohertz via pulsar timing arrays. We study the angular correlation of the timing residuals induced by the spin-2 ultralight dark matter, which is different from the usual Hellings-Downs correlation. At a typical frequency, we show that the spin-2 ultralight dark matter can give rise to the deformation of the Hellings-Downs correlation curve induced by the stochastic gravitational wave background.

## CONTENTS

I. Introduction	1
II. Homogeneous background of spin-2 ULDM	2
III. Pulsar timing residuals induced by spin-2 ULDM	2
IV. Angular correlation curve	3
A. Angular correlation of spin-2 ULDM	3
B. Deformation of Hellings-Downs curve	4
V. Conclusion	4
Acknowledgments	5
A. Theoretical model of spin-2 ULDM	5
References	6

## I. INTRODUCTION

The detection of gravitational waves (GWs) has opened a new era for both theoretical and observational astronomy and cosmology [1]. In different frequency ranges, there exist several different approaches for the detection of GWs [2–5]. With the help of pulsar timing arrays (PTAs), we can detect the signals of stochastic gravitational wave background (SGWB) at frequencies around nanohertz. According to theoretical predictions, there are different physical processes which can contribute to SGWB, including supermassive black hole binaries [6], domain walls [7], scalar curvature perturbations [8], etc.

Compared with other physical effects which may also induce pulsar timing residuals, SGWB has the unique feature that the cross-correlation for different pulsars shows a Hellings-Downs pattern [9], which can help the recognition of SGWB in data analysis.

Recently, several collaborations have reported their newest PTA data analysis independently [10–13], showing the evidence of detection for SGWB. In particular, the cross-correlation pattern resembles the Hellings-Downs correlation, which increases the reliability of the results.

On the other hand, it turns out that ultralight dark matter (ULDM) may also have effects on PTAs [14–20]. ULDM has drawn much attention in recent years. Compared with cold dark matter, ULDM can suppress the structure formation on sub-galactic scales [21]. The oscillation frequency of ULDM is their mass, and for ULDM with mass  $m \sim 10^{-22}$  eV, the corresponding frequency range is around nanohertz. Therefore, the oscillation of gravitational potential induced by ULDM can also induce pulsar timing residuals with particular kind of angular dependence, which may contaminate the Hellings-Downs pattern.

The spin nature of ULDM plays a vital role on its angular correlation on pulsar timing residuals. For example, the scalar ULDM has equal effects on pulsar at each direction [14], while the vector ULDM has strongly anisotropic behaviour [15]. Here we focus on the spin-2 ULDM, which has gained much attention in recent years [22–31]. The theoretical origin of spin-2 ULDM come from the bimetric theory [30]. In the bimetric theory, there are two kinds of gravitons in the mass spectrum, one of which is massless, and the other one is massive. Many efforts have been made to demonstrate that this kind of massive graviton can be a dark matter candidate [22–27].

The spin-2 ULDM has both gravitational effects [19] and coupling effects [16, 17] on PTAs. In this paper, we focus on the couplings effects. We calculate the cross-

\* cairg@itp.ac.cn

† zhangjingrui22@mailsucas.ac.cn

‡ zhangyunlong@nao.cas.cn

correlation of pulsar timing residuals induced by spin-2 ultralight dark matter and the resulting angular pattern is purely quadrupole. We also show that certain parameter choice would cause the Hellings-Downs curve to be slightly or strongly deformed, so the PTA data may help constrain the parameter space.

This paper is organized as follows. In Section II, we show the homogeneous background solution of the spin-2 ULDM. In Section III, we calculate pulsar timing residuals induced by spin-2 ULDM. In Section IV, we evaluate the deformation of spin-2 ULDM on the Hellings-Downs curve, and we summarize the result in Section V. In Appendix A, we overview the bimetric theory and the derivation of massive gravitons.

## II. HOMOGENEOUS BACKGROUND OF SPIN-2 ULDM

The spin-2 ultralight dark matter may come from the bimetric theory [26, 30, 32]. We begin with the following action

$$S_{\text{spin-2}} = \int d^4x \sqrt{|g|} [M_{\text{Pl}}^2 R(g) + \mathcal{L}_M], \quad (1)$$

where the Lagrangian density

$$\mathcal{L}_M = -\frac{1}{2} M^{\mu\nu} \mathcal{E}_{\mu\nu}{}^{\lambda\kappa} M_{\lambda\kappa} - \frac{m^2}{4} (M_{\mu\nu} M^{\mu\nu} - M^2), \quad (2)$$

and the Lichnerowicz operator is given by  $\mathcal{E}_{\mu\nu}{}^{\lambda\kappa} \equiv -\frac{1}{2}(\delta_\mu^\lambda \delta_\nu^\kappa \square - g_{\mu\nu} g^{\lambda\kappa} \square + g^{\lambda\kappa} \nabla_\mu \nabla_\nu + g_{\mu\nu} \nabla^\lambda \nabla^\kappa - 2\nabla^\lambda \nabla_{(\mu} \delta_{\nu)}^\kappa)$ . Since the cosmic expansion is negligible on galactic scales and  $m \gg H$ , we assume the background metric to be flat, so that  $g_{\mu\nu} = \eta_{\mu\nu}$ . The equation of motion for  $M_{\mu\nu}$  from the Lagrangian density is

$$\mathcal{E}_{\mu\nu}{}^{\lambda\kappa} M_{\lambda\kappa} + \frac{1}{2} m^2 (M_{\mu\nu} - \eta_{\mu\nu} M) = 0, \quad (3)$$

where  $M = \eta^{\mu\nu} M_{\mu\nu}$ . Applying  $\partial^\mu$  on (3) gives  $\partial^\mu M_{\mu\nu} = \partial_\nu M$ , and thus  $\partial^\mu \partial^\nu M_{\mu\nu} = \square M$ . Taking trace of (3) and considering  $\eta^{\mu\nu} \mathcal{E}_{\mu\nu}{}^{\lambda\kappa} M_{\lambda\kappa} = 0$ , we can get  $M = 0$ . Then the equation of motion (3) can be rewritten as  $(\square - m^2)M_{\mu\nu} = 0$ . Together we obtain

$$M = 0, \quad \partial^\mu M_{\mu\nu} = 0, \quad (\square - m^2)M_{\mu\nu} = 0. \quad (4)$$

Since the typical velocity of dark matter in the galaxy is  $v/c \sim 10^{-3}$ ,  $M_{00}$  and  $M_{0i}$  component are all suppressed and can be ignored. The homogeneous background solution is then [16]

$$M_{ij} = \frac{\sqrt{2\rho_{\text{DM}}(\mathbf{x})}}{m} \cos(mt + \varphi(\mathbf{x})) \varepsilon_{ij}(\mathbf{x}), \quad (5)$$

where  $\varepsilon_{ij}$  is the polarization tensor,  $\rho_{\text{DM}}(\mathbf{x})$  is the energy density of dark matter at position  $\mathbf{x}$ , and  $\varphi(\mathbf{x})$  represents the phase. Since the occupation number in our galaxy

is  $\frac{\rho_{\text{DM}}}{m \cdot (mv)^3} \approx 10^{95} \left(\frac{\rho_{\text{DM}}}{0.4 \text{ GeV}/\text{cm}^3}\right) \left(\frac{10^{-23} \text{ eV}}{m}\right)^4 \left(\frac{10^{-3}}{v}\right)^3$ , the spin-2 field can be described by a classical wave, and note that the de Broglie wavelength for the spin-2 massive particle with mass  $m$  is

$$\lambda_{\text{DM}} = \frac{2\pi}{mv} \approx 4 \text{ kpc} \left(\frac{10^{-23} \text{ eV}}{m}\right) \left(\frac{10^{-3}}{v}\right), \quad (6)$$

so inhomogeneities within this distance can be smoothed out.

A way to parameterize  $\varepsilon_{ij}$  is to separate it in terms of the spin states [33, 34]

$$\varepsilon_{ij} = \sum_s \varepsilon_s \mathcal{Y}_{ij}^s, \quad (7)$$

where  $s$  represents the 5 different spin states ( $\times, +, \text{L}, \text{R}, \text{S}$ ), with

$$\varepsilon_\times = \varepsilon_{\text{T}} \cos \chi, \quad \varepsilon_+ = \varepsilon_{\text{T}} \sin \chi, \quad (8)$$

$$\varepsilon_{\text{L}} = \varepsilon_{\text{V}} \cos \eta, \quad \varepsilon_{\text{R}} = \varepsilon_{\text{V}} \sin \eta. \quad (9)$$

Here  $\chi$  and  $\eta$  determine the azimuthal direction of tensor part and vector part of the spin-2 field, respectively. Moreover,  $\varepsilon_{\mu\nu}$  is normalized such that

$$\sum_s \varepsilon_s^2 = 1. \quad (10)$$

The corresponding tensors are

$$\mathcal{Y}_{ij}^\times = \frac{1}{\sqrt{2}} (p_i q_j + q_i p_j), \quad (11)$$

$$\mathcal{Y}_{ij}^+ = \frac{1}{\sqrt{2}} (p_i p_j - q_i q_j), \quad (12)$$

$$\mathcal{Y}_{ij}^{\text{L}} = \frac{1}{\sqrt{2}} (q_i r_j + r_i q_j), \quad (13)$$

$$\mathcal{Y}_{ij}^{\text{R}} = \frac{1}{\sqrt{2}} (p_i r_j + r_i p_j), \quad (14)$$

$$\mathcal{Y}_{ij}^{\text{S}} = \frac{1}{\sqrt{6}} (3r_i r_j - \delta_{ij}), \quad (15)$$

which represent -2, 2, -1, 1, 0 spin states, respectively,  $r_i$  is the unit vector with propagation direction of the massive spin-2 field, and  $p_i, q_i$  are two unit vectors orthogonal to  $r_i$  and to each other. Note that in general, spin-2 fields can have at most 6 degrees of freedom, while in the case of bimetric theory [26], the traceless condition restricts the number to 5.

## III. PULSAR TIMING RESIDUALS INDUCED BY SPIN-2 ULDM

To study the effects on the PTA signal, a convenient way to calculate is to change the frame as in [16],  $\tilde{g}_{\mu\nu} = g_{\mu\nu} - \frac{\alpha}{M_{\text{Pl}}} M_{\mu\nu}$ , and evaluate the geodesics of photons

based on the new metric  $\tilde{g}_{\mu\nu}$ . Here we assume a flat background since  $m \gg H$  and work with  $\tilde{g}_{ij} = \delta_{ij} - \frac{\alpha}{M_{\text{Pl}}} M_{ij}$ . For a photon travelling along the geodesic from the pulsar  $a$  to the Earth with 4-momentum  $p^\mu = \nu(1, n_a^i)$ , the geodesic equation gives

$$\frac{dp^0}{du} = \frac{\alpha\nu^2}{2M_{\text{Pl}}} \partial_t M_{ij} n_a^i n_a^j, \quad (16)$$

where  $u$  is the affine parameter. Treating  $\alpha$  as a small parameter and keeping first order terms in  $\alpha$ , we get

$$\nu = \bar{\nu} \left( 1 + \frac{\alpha}{2M_{\text{Pl}}} \int_a^{\text{E}} du \bar{\nu} \partial_t M_{ij} n_a^i n_a^j \right), \quad (17)$$

where the integral is evaluated from the pulsar  $a$  to the Earth(E), and  $\bar{\nu}$  is the frequency of the photon if not perturbed.

By making use of  $\bar{\nu} \partial_t = \frac{d}{du} - \bar{\nu} n_a^i \partial_i$ , it becomes

$$\begin{aligned} \nu &= \bar{\nu} \left( 1 + \frac{\alpha}{2M_{\text{Pl}}} (M_{ij}^{\text{E}} - M_{ij}^a) n_a^i n_a^j - \right. \\ &\quad \left. \frac{\alpha}{2M_{\text{Pl}}} \int_a^{\text{E}} du \nu_0 n^k \partial_k M_{ij} n_a^i n_a^j \right). \end{aligned} \quad (18)$$

Compared with the second term, the last term can be ignored since it contains space derivatives which introduce a factor  $v/c \sim \mathcal{O}(10^{-3})$ . The resulting redshift  $z_a = (\bar{\nu}_a - \nu_a)/\bar{\nu}_a$  for signals from the pulsar  $a$  is

$$\begin{aligned} z_a &= -\frac{\alpha}{2M_{\text{Pl}}} (M_{ij}^{\text{E}} - M_{ij}^a) n_a^i n_a^j \\ &= F_a^{\text{E}} \Psi_o(\mathbf{x}_{\text{E}}) \cos(mt + \varphi_{\text{E}}) \\ &\quad - F_a^{\text{P}} \Psi_o(\mathbf{x}_a) \cos(mt - mL_a + \varphi_a), \end{aligned} \quad (19)$$

where  $L_a$  is the distance between the pulsar  $a$  and the Earth, and the corresponding beam pattern functions are

$$F_a^{\text{E}} = -\varepsilon_{ij}(\mathbf{x}_{\text{E}}) n_a^i n_a^j, \quad (20)$$

$$F_a^{\text{P}} = -\varepsilon_{ij}(\mathbf{x}_a) n_a^i n_a^j, \quad (21)$$

which contain the dependence of  $z_a$  on angles, while

$$\Psi_o(\mathbf{x}_{\text{E}}) = \frac{\alpha \sqrt{\rho_{\text{DM}}(\mathbf{x}_{\text{E}})}}{\sqrt{2} m M_{\text{Pl}}}, \quad (22)$$

$$\Psi_o(\mathbf{x}_a) = \frac{\alpha \sqrt{\rho_{\text{DM}}(\mathbf{x}_a)}}{\sqrt{2} m M_{\text{Pl}}}, \quad (23)$$

represent the amplitude of  $z_a$ , which depends on local energy density of dark matter.

The timing residuals

$$\Delta T_a(t) = \int_0^t dt' z_a(t') \quad (24)$$

are then integrated to be

$$\begin{aligned} \Delta T_a(t) &= \frac{1}{m} [F_a^{\text{E}} \Psi_o(\mathbf{x}_{\text{E}}) \sin(mt + \varphi_{\text{E}}) + \\ &\quad - F_a^{\text{P}} \Psi_o(\mathbf{x}_a) \sin(mt - mL_a + \varphi_a)], \end{aligned} \quad (25)$$

with origin of time chosen to cancel constant terms for simplicity.

#### IV. ANGULAR CORRELATION CURVE

For pulsar  $a$  and pulsar  $b$ , the cross-correlation between their timing residuals can be written as

$$C_{ab}(\tau) = \langle \Delta T_a(t) \Delta T_b(t + \tau) \rangle - \langle \Delta T_a(t) \rangle \langle \Delta T_b(t + \tau) \rangle. \quad (26)$$

For the stochastic gravitational wave background, the cross-correlation it induces can be described by [9, 20]

$$C_{ab}^{\text{GW}}(\tau) = \sum_i \Gamma_{\text{HD}}(\zeta) \Phi_{\text{GW}}(f_i) \cos 2\pi f_i \tau, \quad (27)$$

where  $\Gamma_{\text{HD}}$  describes the Helling-Downs curve

$$\begin{aligned} \Gamma_{\text{HD}} &= \frac{1}{2} - \frac{1}{4} \left( \frac{1 - \cos \zeta}{2} \right) + \\ &\quad + \frac{3}{2} \left( \frac{1 - \cos \zeta}{2} \right) \ln \left( \frac{1 - \cos \zeta}{2} \right), \end{aligned} \quad (28)$$

and

$$\Phi_{\text{GW}}(f_i) = \frac{1}{12\pi^2 f_i^3} \frac{1}{T_{\text{obs}}} h_c^2(f_i). \quad (29)$$

The frequency integral is discretized based on the observation time  $T_{\text{obs}}$  [10], and  $h_c$  is the characteristic strain of SGWB, which usually can be parameterized as

$$h_c(f) = A_{\text{GW}} \left( \frac{f}{f_0} \right)^\alpha. \quad (30)$$

##### A. Angular correlation of spin-2 ULDM

Notice that, for ultralight dark matter with mass  $m \gtrsim 10^{-24} \text{eV}$ , the observational period for pulsars is  $T_{\text{obs}} \sim 10 \text{yr}$ . When we take the time average, the terms with  $\cos(mt)$  vanish. Using the timing residuals in (25), the non-vanishing cross-correlation terms are

$$\begin{aligned} &\langle \Delta T_a(t) \Delta T_b(t + \tau) \rangle \\ &= \frac{1}{2m^2} \langle F_a^{\text{E}} F_b^{\text{E}} \rangle \langle \Psi_o^2(\mathbf{x}_{\text{E}}) \rangle \cos(m\tau) \\ &\quad + \frac{1}{2m^2} \langle F_a^{\text{P}} F_b^{\text{P}} \rangle \langle \Psi_o(\mathbf{x}_a) \Psi_o(\mathbf{x}_b) \rangle \\ &\quad \quad \times \cos(m\tau + mL_a - mL_b - \Upsilon_a + \Upsilon_b) \\ &\quad - \frac{1}{2m^2} \langle F_a^{\text{E}} F_b^{\text{P}} \rangle \langle \Psi_o(\mathbf{x}_{\text{E}}) \Psi_o(\mathbf{x}_b) \rangle \\ &\quad \quad \times \cos(m\tau - mL_b + \Upsilon_b - \Upsilon_{\text{E}}) \\ &\quad - \frac{1}{2m^2} \langle F_a^{\text{P}} F_b^{\text{E}} \rangle \langle \Psi_o(\mathbf{x}_{\text{E}}) \Psi_o(\mathbf{x}_a) \rangle \\ &\quad \quad \times \cos(m\tau + mL_a + \Upsilon_{\text{E}} - \Upsilon_a). \end{aligned} \quad (31)$$

While except the first term, all other terms are averaged to zero after evaluating the distance between different pulsars and the Earth. Thus, the final result is

$$C_{ab}^{\text{spin-2}}(\tau) \approx \frac{1}{2m^2} \langle F_a^{\text{E}} F_b^{\text{E}} \rangle \langle \Psi_o^2(\mathbf{x}_{\text{E}}) \rangle \cos(m\tau). \quad (32)$$

The angular dependence of  $C_{ab}^{\text{spin-2}}$  is contained in  $\langle F_a^E F_b^E \rangle$ , we set the coordinate frame in which  $n_a^i = (0, 0, 1)$  and  $n_b^i = (\sin \zeta, 0, \cos \zeta)$ . Since observable pulsars are distributed all over the sky, effectively, we can assume the polarization for the massive spin-2 field as isotropic and integrate over possible directions [20] and also integrate over azimuthal directions of tensor and vector parts. For convenience, we set

$$\vec{r} = (\sin \theta \cos \phi, \sin \theta \sin \phi, \cos \theta), \quad (33)$$

$$\vec{p} = (\sin \phi, -\cos \phi, 0), \quad (34)$$

$$\vec{q} = (\cos \theta \cos \phi, \cos \theta \sin \phi, -\sin \theta). \quad (35)$$

The Hellings-Downs-like curve for massive spin-2 background can be derived from  $\varepsilon_{ij} n^i n^j$ ,

$$\begin{aligned} \langle F_a^E F_b^E \rangle &= \int \frac{d\eta}{2\pi} \frac{d\chi}{2\pi} \frac{d^2\Omega}{4\pi} \sum_s \varepsilon_s \mathcal{Y}_{ij}^s n_a^i n_a^j \sum_\lambda \varepsilon_\lambda \mathcal{Y}_{kl}^\lambda n_b^k n_b^l \\ &= \frac{1}{30} (1 + 3 \cos 2\zeta) = \frac{4}{15} \Gamma_{\text{DM}}(\zeta), \end{aligned} \quad (36)$$

where

$$\Gamma_{\text{DM}}(\zeta) = \frac{1}{2} P_2(\cos \zeta) = \frac{1}{8} (1 + 3 \cos 2\zeta) \quad (37)$$

is the angular correlation curve normalized to be compared with Hellings-Downs curve in Figure 1. Here we can see that the effect of spin-2 ultralight dark matter follows a purely quadrupole pattern.

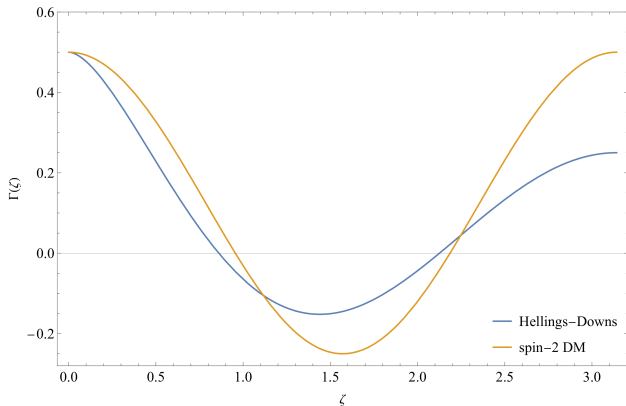


FIG. 1. The blue and orange curves represent the angular correlation of the timing residuals induced by stochastic GW background (Hellings-Downs curve) and spin-2 ultralight dark matter, respectively. Both curves are normalized at  $\zeta = 0$  such that  $\Gamma(0) = 1/2$ .

The total result for the correlation is

$$C_{ab}^{\text{DM}}(\tau) = \Phi_{\text{DM}} \Gamma_{\text{DM}}(\zeta) \cos(m\tau), \quad (38)$$

where  $\Phi_{\text{DM}}$  denotes the amplitude of the correlation

$$\Phi_{\text{DM}} = \frac{2}{15m^2} \langle \Psi_0^2(\mathbf{x}_E) \rangle. \quad (39)$$

## B. Deformation of Hellings-Downs curve

When SGWB and spin-2 ultralight dark matter are both considered, the total cross-correlation is

$$\begin{aligned} C_{ab}(\tau) &= \sum_i \Gamma_{\text{HD}}(\zeta) \Phi_{\text{GW}}(f_i) \cos 2\pi f_i \tau \\ &\quad + \Gamma_{\text{DM}}(\zeta) \Phi_{\text{DM}} \cos(2\pi f_m \tau), \end{aligned} \quad (40)$$

where the effect of spin-2 ultralight dark matter at frequency  $f_m = m/2\pi$  can be incorporated into  $\Gamma(\zeta)$  as [20]

$$\begin{aligned} \Gamma_{\text{eff}}(\zeta) &= \frac{\Phi_{\text{GW}}(m/2\pi)}{\Phi_{\text{GW}}(m/2\pi) + \Phi_{\text{DM}}} \Gamma_{\text{HD}}(\zeta) + \\ &\quad \frac{\Phi_{\text{DM}}}{\Phi_{\text{GW}}(m/2\pi) + \Phi_{\text{DM}}} \Gamma_{\text{DM}}(\zeta). \end{aligned} \quad (41)$$

In the case of SGWB, according to the observation of NANOGrav reported in [10], for  $\gamma = 13/3$ ,  $A_{\text{GW}} = 2.4 \times 10^{-15}$  with the observation time  $T_{\text{obs}} \sim 15$  yr and  $f_{\text{ref}} = 1$  yr $^{-1}$ , so the amplitude of the correlation is

$$\Phi_{\text{GW}}(m/2\pi) \sim 1 \times 10^{-32} \text{yr}^2 \left( \frac{m}{10^{-22} \text{eV}} \right)^{-\frac{13}{3}} \left( \frac{15 \text{yr}}{T_{\text{obs}}} \right). \quad (42)$$

For the effects of ultralight dark matter, the amplitude of correlation can be derived from (22) and (39) as

$$\Phi_{\text{DM}} = \frac{\alpha^2}{15m^4} \frac{\rho_{\text{DM}}(\mathbf{x}_E)}{M_{\text{Pl}}^2}, \quad (43)$$

so that

$$\begin{aligned} \Phi_{\text{DM}} &\sim 6 \times 10^{-33} \text{yr}^2 \left( \frac{\rho_{\text{DM}}}{0.4 \text{GeV}/\text{cm}^3} \right) \\ &\quad \times \left( \frac{\alpha}{10^{-6}} \right)^2 \left( \frac{m}{10^{-22} \text{eV}} \right)^{-4}. \end{aligned} \quad (44)$$

Different choices of the parameters  $\alpha$  and  $m$  give different deformations of the Hellings-Downs curve, shown in Fig. 2, Fig. 3 and Fig. 4. It can be seen from these figures that, compared with the mass of dark matter  $m$ , the order of magnitude of the coupling constant  $\alpha$  has significant impact on the deformation of the Hellings-Downs curve at certain frequencies. For example, for  $\alpha > 10^{-5}$ , the shape of the curve is almost determined by the spin-2 ultralight dark matter. It is also interesting that with smaller mass parameter of the ultralight dark matter, the deformation is larger and easier to be observed.

## V. CONCLUSION

In summary, we show that spin-2 ultralight dark matter can induce deformation of Hellings-Downs curve at the frequency of the mass parameter. Since the residuals induced by spin-2 ultralight dark matter is monochromatic, the deformation of Hellings-Downs curve is expected to happen only in a narrow frequency range

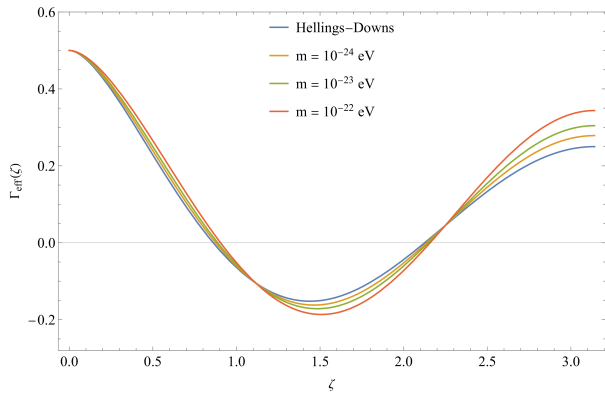


FIG. 2. Effective cross-correlation curves with  $\alpha = 10^{-6}$  and mass ranging from  $10^{-24}$  eV to  $10^{-22}$  eV. It can be seen that in this range and at the typical frequencies  $f_m = m/2\pi$ , the deformation of spin-2 ultralight dark matter on the Hellings-Downs curve is relatively small.

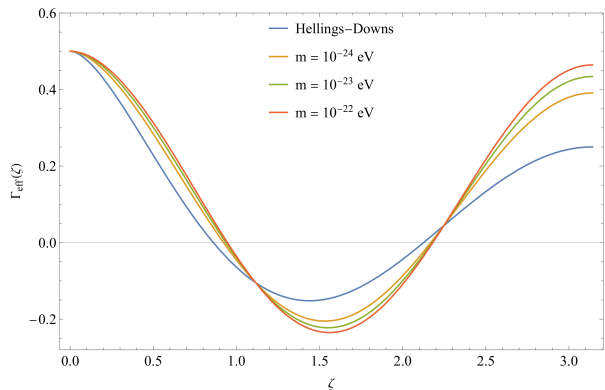


FIG. 3. Effective cross-correlation curves with  $\alpha = 10^{-5.5}$  and mass ranging from  $10^{-24}$  eV to  $10^{-22}$  eV. The deformation is very strong in this parameter range, suggesting that if the coupling constant  $\alpha$  is above this magnitude, existing ultralight spin-2 ultralight dark matter would have considerable effects on the deformation of the Hellings-Downs curve at the typical frequencies  $f_m = m/2\pi$ .

around  $f = m/2\pi$ . Both the mass of spin-2 ultralight dark matter and the coupling constant  $\alpha$  have impact on the deformation, so the observational data of PTAs can help to constrain the parameter space.

Comparing with the spin-1 case in [20], the spin-2 ultralight dark matter has a pure quadrupole effect on the correlation, which is expected from its tensorial nature. According to PTA data [19], the coupling constant  $\alpha$  is constrained at  $10^{-6} \sim 10^{-5}$  for mass  $m < 5 \times 10^{-23}$  eV. The constraint is set merely according to the amplitude of gravitational strain. The angular correlation we have found gives a more concrete understanding on how the spin-2 ultralight dark matter can affect the PTA signal, causing angular correlation of the timing residuals, and deforming the correlation curve of stochastic gravitational wave background.

The spin-2 ultralight dark matter have different effects

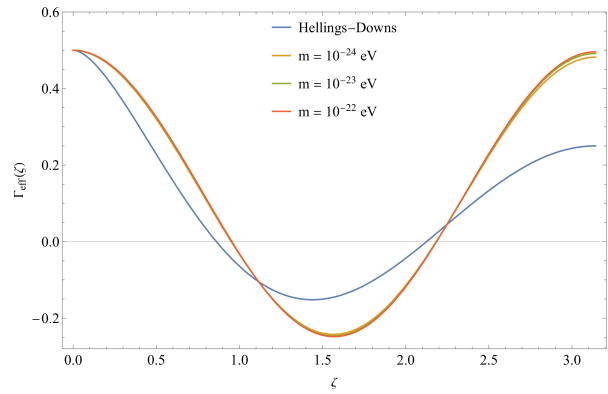


FIG. 4. Effective cross-correlation curves with  $\alpha = 10^{-5}$  and mass ranging from  $10^{-24}$  eV to  $10^{-22}$  eV. In this range of  $\alpha$ , the curves are dominated by the spin-2 ultralight dark matter at the typical frequencies  $f_m = m/2\pi$ .

on pulsar timing residuals, compared with the stochastic GW background. The PTA residuals are induced by the local homogeneous background from pulsars to the Earth, and the Hellings-Downs curve is caused by isotropic gravitational waves coming from all over the space. The spin-2 ultralight dark matter is massive, which makes the frequency of the homogeneous background fixed to its mass.

Our results can be used to give a intuitive comparison with experimental data, and estimate the constraint on spin-2 ultralight dark matter. Experimentally, if apparent deformation of Hellings-Downs curve is observed in certain frequency range, it can be compared with our results to verify if the deformation is caused by the spin-2 ultralight dark matter. In this sense, PTAs act as an distinct dark matter detection experiment for spin-2 ultralight dark matter. In the future, we may combine the theoretical model with the observational data of PTAs and further analyze the effects of spin-2 ultralight dark matter on PTAs.

## ACKNOWLEDGMENTS

This work is supported by the National Key Research and Development Program of China (Grants No. 2021YFA078304, No.2021YFC2201901) and the National Natural Science Foundation of China (Grants No. 12375059, No.12235019, No.11991052, No.11947302, and No.11821505).

## Appendix A: Theoretical model of spin-2 ULDM

The theory of massive spin-2 ultralight dark matter can originate from bimetric theory [26, 30, 32], which was constructed originally in order to generalize Fierz-Pauli massive gravity in a non-linear way. Later it was found that this theory could provide a reasonable origin for spin-2 ultralight dark matter [22, 23, 26]. The total

action is given by

$$S = \frac{M_{\text{Pl}}^2}{1 + \alpha^2} \int d^4x \left[ \sqrt{|\tilde{g}|} R(\tilde{g}) + \alpha^2 \sqrt{|f|} R(f) - 2 \frac{\alpha^2 M_{\text{Pl}}^2}{1 + \alpha^2} \sqrt{|\tilde{g}|} V(\tilde{g}, f; \beta_n) \right] + \int d^4x \sqrt{|\tilde{g}|} \mathcal{L}_m(\tilde{g}, \Psi), \quad (\text{A1})$$

where  $M_{\text{Pl}}$  is the reduced Planck mass,  $f_{\mu\nu}$  is introduced as a new spin-2 field, while  $\alpha$  is a dimensionless constant to regulate the difference of interactions for two spin-2 fields, and  $V(\tilde{g}, f; \beta_n)$  stands for interaction terms between the two fields in order to avoid ghosts [23, 30, 32]. This action can be linearized by considering perturbations

$$\tilde{g}_{\mu\nu} = \bar{g}_{\mu\nu} + \frac{1}{M_{\text{Pl}}} (\mathcal{G}_{\mu\nu} - \alpha M_{\mu\nu}), \quad (\text{A2})$$

$$f_{\mu\nu} = \bar{g}_{\mu\nu} + \frac{1}{M_{\text{Pl}}} (\mathcal{G}_{\mu\nu} + \alpha^{-1} M_{\mu\nu}), \quad (\text{A3})$$

where  $\bar{g}_{\mu\nu}$  is the background metric,  $\mathcal{G}_{\mu\nu}$  and  $M_{\mu\nu}$  are the small perturbations. Furthermore, the resulting action can be diagonalized by this linear combination of the two metric perturbations. Then the quadratic part of the total action (A1) becomes

$$S^{(2)} = \int d^4x \sqrt{|\bar{g}|} \left[ \mathcal{L}_{\text{GR}}^{(2)}(\mathcal{G}) + \mathcal{L}_{\text{FP}}^{(2)}(M) + \frac{1}{M_{\text{Pl}}} (\mathcal{G}_{\mu\nu} - \alpha M_{\mu\nu}) T^{\mu\nu}(\Psi) \right], \quad (\text{A4})$$

where  $\mathcal{L}_{\text{GR}}^{(2)}(X)$  is 2nd-order perturbation expansion of Einstein-Hilbert action, described by the Lichnerowicz operator, as

$$\begin{aligned} \mathcal{L}_{\text{GR}}^{(2)}(X) &= -\frac{1}{2} M_{\text{Pl}}^2 X^{\mu\nu} \mathcal{E}_{\mu\nu}{}^{\lambda\kappa} X_{\lambda\kappa} \\ &= -\frac{1}{4} M_{\text{Pl}}^2 X^{\mu\nu} \left( \delta_{\mu}^{\lambda} \delta_{\nu}^{\kappa} \square - \bar{g}_{\mu\nu} \bar{g}^{\lambda\kappa} \square + \bar{g}^{\lambda\kappa} \nabla_{\mu} \nabla_{\nu} + \bar{g}_{\mu\nu} \nabla^{\lambda} \nabla^{\kappa} - 2 \nabla^{\lambda} \nabla_{(\mu} \delta_{\nu)}^{\kappa} \right) X_{\lambda\kappa}, \end{aligned} \quad (\text{A5})$$

while  $\mathcal{L}_{\text{FP}}^{(2)}(M)$  represents the Fierz-Pauli Lagrangian, which describes a massive spin-2 field

$$\mathcal{L}_{\text{FP}}^{(2)}(M) = \mathcal{L}_{\text{GR}}^{(2)}(M) - \frac{m^2}{4} (M_{\mu\nu} M^{\mu\nu} - M^2), \quad (\text{A6})$$

and  $m = \sqrt{\beta_1 + 2\beta_2 + \beta_3} M_{\text{Pl}}$  can be identified as the mass for the mass eigenstate  $M_{\mu\nu}$ . Terms in  $\mathcal{G}_{\mu\nu}$  can be combined with background metric  $g_{\mu\nu} = \bar{g}_{\mu\nu} + \frac{1}{M_{\text{Pl}}} \mathcal{G}_{\mu\nu}$  and re-summed to recover Einstein-Hilbert action. The resulting total action is

$$S_{\text{spin-2}} = M_{\text{Pl}}^2 \int d^4x \sqrt{|g|} \left[ R(g) + \mathcal{L}_{\text{FP}}^{(2)}(M) + \mathcal{O}(M_{\mu\nu}^3) \right]. \quad (\text{A7})$$

- 
- [1] B. P. Abbott *et al.* [LIGO Scientific and Virgo], ‘‘Observation of Gravitational Waves from a Binary Black Hole Merger,’’ *Phys. Rev. Lett.* **116**, no.6, 061102 (2016) doi:10.1103/PhysRevLett.116.061102 [arXiv:1602.03837 [gr-qc]].
- [2] J. Aasi *et al.* [LIGO Scientific], ‘‘Advanced LIGO,’’ *Class. Quant. Grav.* **32**, 074001 (2015) doi:10.1088/0264-9381/32/7/074001 [arXiv:1411.4547 [gr-qc]].
- [3] F. Acernese *et al.* [VIRGO], ‘‘Advanced Virgo: a second-generation interferometric gravitational wave detector,’’ *Class. Quant. Grav.* **32**, no.2, 024001 (2015) doi:10.1088/0264-9381/32/2/024001 [arXiv:1408.3978 [gr-qc]].
- [4] P. Amaro-Seoane *et al.* [LISA], ‘‘Laser Interferometer Space Antenna,’’ [arXiv:1702.00786 [astro-ph.IM]].
- [5] W. H. Ruan, Z. K. Guo, R. G. Cai and Y. Z. Zhang, ‘‘Taiji program: Gravitational-wave sources,’’ *Int. J. Mod. Phys. A* **35**, no.17, 2050075 (2020) doi:10.1142/S0217751X2050075X [arXiv:1807.09495 [gr-qc]].
- [6] S. Burke-Spolaor, S. R. Taylor, M. Charisi, T. Dolch, J. S. Hazboun, A. M. Holgado, L. Z. Kelley, T. J. W. Lazio, D. R. Madison and N. McMann, *et al.* ‘‘The Astrophysics of Nanohertz Gravitational Waves,’’ *Astron. Astrophys. Rev.* **27**, no.1, 5 (2019) doi:10.1007/s00159-019-0115-7 [arXiv:1811.08826 [astro-ph.HE]].
- [7] Z. Zhang, C. Cai, Y. H. Su, S. Wang, Z. H. Yu and H. H. Zhang, ‘‘Nano-Hertz gravitational waves from collapsing domain walls associated with freeze-in dark matter in light of pulsar timing array observations,’’ [arXiv:2307.11495 [hep-ph]].
- [8] S. Balaji, G. Domènech and G. Franciolini, ‘‘Scalar-induced gravitational wave interpretation of PTA data: the role of scalar fluctuation propagation speed,’’ *JCAP* **10**, 041 (2023) doi:10.1088/1475-7516/2023/10/041 [arXiv:2307.08552 [gr-qc]].
- [9] R. w. Hellings and G. s. Downs, ‘‘UPPER LIMITS ON THE ISOTROPIC GRAVITATIONAL RADIATION BACKGROUND FROM PULSAR TIMING ANALYSIS,’’ *Astrophys. J. Lett.* **265**, L39-L42 (1983) doi:10.1086/183954
- [10] G. Agazie *et al.* [NANOGrav], ‘‘The NANOGrav 15 yr Data Set: Evidence for a Gravitational-wave Background,’’ *Astrophys. J. Lett.* **951**, no.1, L8 (2023) doi:10.3847/2041-8213/acdac6 [arXiv:2306.16213 [astro-ph.HE]].
- [11] J. Antoniadis *et al.* [EPTA], ‘‘The second data release from the European Pulsar Timing Array III. Search for gravitational wave signals,’’ *Astron. Astrophys.* **678**, A50 (2023) doi:10.1051/0004-6361/202346844 [arXiv:2306.16214 [astro-ph.HE]].
- [12] D. J. Reardon, A. Zic, R. M. Shannon, G. B. Hobbs, M. Bailes, V. Di Marco, A. Kapur, A. F. Rogers,

- E. Thrane and J. Askew, *et al.* “Search for an Isotropic Gravitational-wave Background with the Parkes Pulsar Timing Array,” *Astrophys. J. Lett.* **951**, no.1, L6 (2023) doi:10.3847/2041-8213/acdd02 [arXiv:2306.16215 [astro-ph.HE]].
- [13] H. Xu, S. Chen, Y. Guo, J. Jiang, B. Wang, J. Xu, Z. Xue, R. N. Caballero, J. Yuan and Y. Xu, *et al.* “Searching for the Nano-Hertz Stochastic Gravitational Wave Background with the Chinese Pulsar Timing Array Data Release I,” *Res. Astron. Astrophys.* **23**, no.7, 075024 (2023) doi:10.1088/1674-4527/acdfa5 [arXiv:2306.16216 [astro-ph.HE]].
- [14] A. Khmelnitsky and V. Rubakov, “Pulsar timing signal from ultralight scalar dark matter,” *JCAP* **02**, 019 (2014) doi:10.1088/1475-7516/2014/02/019 [arXiv:1309.5888 [astro-ph.CO]].
- [15] K. Nomura, A. Ito and J. Soda, “Pulsar timing residual induced by ultralight vector dark matter,” *Eur. Phys. J. C* **80**, no.5, 419 (2020) doi:10.1140/epjc/s10052-020-7990-y [arXiv:1912.10210 [gr-qc]].
- [16] J. M. Armaleo, D. López Nacir and F. R. Urban, “Pulsar timing array constraints on spin-2 ULDM,” *JCAP* **09**, 031 (2020) doi:10.1088/1475-7516/2020/09/031 [arXiv:2005.03731 [astro-ph.CO]].
- [17] S. Sun, X. Y. Yang and Y. L. Zhang, “Pulsar timing residual induced by wideband ultralight dark matter with spin 0,1,2,” *Phys. Rev. D* **106**, no.6, 066006 (2022) doi:10.1103/PhysRevD.106.066006 [arXiv:2112.15593 [astro-ph.CO]].
- [18] C. Unal, F. R. Urban and E. D. Kovetz, “Probing ultralight scalar, vector and tensor dark matter with pulsar timing arrays,” [arXiv:2209.02741 [astro-ph.CO]].
- [19] Y. M. Wu, Z. C. Chen and Q. G. Huang, “Pulsar timing residual induced by ultralight tensor dark matter,” *JCAP* **09**, 021 (2023) doi:10.1088/1475-7516/2023/09/021 [arXiv:2305.08091 [hep-ph]].
- [20] H. Omiya, K. Nomura and J. Soda, “Hellings-Downs curve deformed by ultralight vector dark matter,” *Phys. Rev. D* **108**, no.10, 104006 (2023) doi:10.1103/PhysRevD.108.104006 [arXiv:2307.12624 [astro-ph.CO]].
- [21] E. G. M. Ferreira, “Ultra-light dark matter,” *Astron. Astrophys. Rev.* **29**, no.1, 7 (2021) doi:10.1007/s00159-021-00135-6 [arXiv:2005.03254 [astro-ph.CO]].
- [22] K. Aoki and S. Mukohyama, “Massive gravitons as dark matter and gravitational waves,” *Phys. Rev. D* **94**, no.2, 024001 (2016) doi:10.1103/PhysRevD.94.024001 [arXiv:1604.06704 [hep-th]].
- [23] E. Babichev, L. Marzola, M. Raidal, A. Schmidt-May, F. Urban, H. Veermäe and M. von Strauss, “Bigravitational origin of dark matter,” *Phys. Rev. D* **94**, no.8, 084055 (2016) doi:10.1103/PhysRevD.94.084055 [arXiv:1604.08564 [hep-ph]].
- [24] E. Babichev, L. Marzola, M. Raidal, A. Schmidt-May, F. Urban, H. Veermäe and M. von Strauss, “Heavy spin-2 ultralight dark matter,” *JCAP* **09**, 016 (2016) doi:10.1088/1475-7516/2016/09/016 [arXiv:1607.03497 [hep-th]].
- [25] K. Aoki and K. i. Maeda, “Condensate of Massive Graviton and Dark Matter,” *Phys. Rev. D* **97**, no.4, 044002 (2018) doi:10.1103/PhysRevD.97.044002 [arXiv:1707.05003 [hep-th]].
- [26] L. Marzola, M. Raidal and F. R. Urban, “Oscillating spin-2 ultralight dark matter,” *Phys. Rev. D* **97**, no.2, 024010 (2018) doi:10.1103/PhysRevD.97.024010 [arXiv:1708.04253 [hep-ph]].
- [27] Y. Manita, K. Aoki, T. Fujita and S. Mukohyama, “spin-2 ultralight dark matter from an anisotropic universe in bigravity,” *Phys. Rev. D* **107**, no.10, 104007 (2023) doi:10.1103/PhysRevD.107.104007 [arXiv:2211.15873 [gr-qc]].
- [28] E. W. Kolb, S. Ling, A. J. Long and R. A. Rosen, “Cosmological gravitational particle production of massive spin-2 particles,” *JHEP* **05**, 181 (2023) doi:10.1007/JHEP05(2023)181 [arXiv:2302.04390 [astro-ph.CO]].
- [29] M. A. Gorji, “spin-2 ultralight dark matter from inflation,” [arXiv:2305.13381 [astro-ph.CO]].
- [30] S. F. Hassan and R. A. Rosen, “Bimetric Gravity from Ghost-free Massive Gravity,” *JHEP* **02**, 126 (2012) doi:10.1007/JHEP02(2012)126 [arXiv:1109.3515 [hep-th]].
- [31] R. Z. Guo, Y. Jiang and Q. G. Huang, “Probing Ultralight Tensor Dark Matter with the Stochastic Gravitational-Wave Background from Advanced LIGO and Virgo’s First Three Observing Runs,” [arXiv:2312.16435 [astro-ph.CO]].
- [32] A. Schmidt-May and M. von Strauss, “Recent developments in bimetric theory,” *J. Phys. A* **49**, no.18, 183001 (2016) doi:10.1088/1751-8113/49/18/183001 [arXiv:1512.00021 [hep-th]].
- [33] J. M. Armaleo, D. López Nacir and F. R. Urban, “Binary pulsars as probes for spin-2 ultralight dark matter,” *JCAP* **01**, 053 (2020) doi:10.1088/1475-7516/2020/01/053 [arXiv:1909.13814 [astro-ph.HE]].
- [34] J. M. Armaleo, D. López Nacir and F. R. Urban, “Searching for spin-2 ULDM with gravitational waves interferometers,” *JCAP* **04**, 053 (2021) doi:10.1088/1475-7516/2021/04/053 [arXiv:2012.13997 [astro-ph.CO]].